

AD-A207 385 ELECTRON-IMPACT IONIZATION TIME-OF-FLIGHT MASS
SPECTROMETER FOR MOLECULAR. (U) AEROSPACE CORP EL
SEGUNDO CA AEROPHYSICS LAB J E POLLARD ET AL.

1/1

UNCLASSIFIED 15 APR 89 TR-0086(6908)-1 SD-TR-89-25 F/G 7/4

NL



AD-A207 385
1/1
F/G 7/4



UTION TEST CHART

DTIC FILE COPY

Electron-Impact Ionization Time-of-Flight Mass Spectrometer for Molecular Beams

J. E. POLLARD and R. B. COHEN
Aerophysics Laboratory
Laboratory Operations
The Aerospace Corporation
El Segundo, CA 90245

15 April 1989

Prepared for

SPACE SYSTEMS DIVISION
AIR FORCE SYSTEMS COMMAND
Los Angeles Air Force Base
P.O. Box 92960
Los Angeles, CA 90009-2960

APPROVED FOR PUBLIC RELEASE;
DISTRIBUTION UNLIMITED

DTIC
ELECTE
MAY 11 1989
S H D

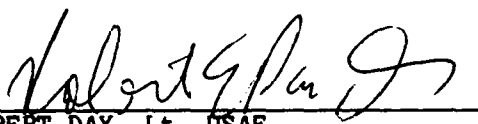
AD-A207 585

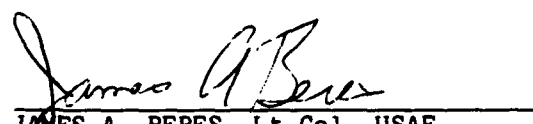
89 5 11 130

This report was submitted by The Aerospace Corporation, El Segundo, CA 90245, under Contract No. F04701-85-C-0086 with the Space Systems Division, P.O. Box 92960, Los Angeles, CA 90009-2960. It was reviewed and approved for The Aerospace Corporation by W. P. Thompson, Director, Aerophysics Laboratory. Lt Robert Day, SD/CLUE was the project officer.

This report has been reviewed by the Public Affairs Office (PAS) and is releasable to the National Technical Information Service (NTIS). At NTIS, it will be available to the general public, including foreign nationals.

This technical report has been reviewed and is approved for publication. Publication of this report does not constitute Air Force approval of the report's findings or conclusions. It is published only for the exchange and stimulation of ideas.


ROBERT DAY, Lt, USAF
Project Officer
SD/CLUE


JAMES A. BERES, Lt Col, USAF
Director, AFSTC West Coast Office
AFSTC/WCO

REPORT DOCUMENTATION PAGE

1a. REPORT SECURITY CLASSIFICATION Unclassified			1b. RESTRICTIVE MARKINGS	
2a. SECURITY CLASSIFICATION AUTHORITY			3. DISTRIBUTION / AVAILABILITY OF REPORT Approved for public release; distribution unlimited.	
2b. DECLASSIFICATION / DOWNGRADING SCHEDULE				
4. PERFORMING ORGANIZATION REPORT NUMBER(S) TR-0086(6908)-1			5. MONITORING ORGANIZATION REPORT NUMBER(S) SD-TR-89-25	
6a. NAME OF PERFORMING ORGANIZATION The Aerospace Corporation Laboratory Operations		6b. OFFICE SYMBOL (If applicable)	7a. NAME OF MONITORING ORGANIZATION Space Systems Division	
6c. ADDRESS (City, State, and ZIP Code) E1 Segundo, CA 90245		7b. ADDRESS (City, State, and ZIP Code) Los Angeles Air Force Base Los Angeles, CA 90009-2960		
8a. NAME OF FUNDING / SPONSORING ORGANIZATION		8b. OFFICE SYMBOL (If applicable)	9. PROCUREMENT INSTRUMENT IDENTIFICATION NUMBER F04701-85-C-0086	
8c. ADDRESS (City, State, and ZIP Code)		10. SOURCE OF FUNDING NUMBERS		
		PROGRAM ELEMENT NO.	PROJECT NO.	TASK NO.
				WORK UNIT ACCESSION NO.
11. TITLE (Include Security Classification) Electron-Impact Ionization Time-of-Flight Mass Spectrometer for Molecular Beams				
12. PERSONAL AUTHOR(S) Pollard, James E.; and Cohen, Ronald B.				
13a. TYPE OF REPORT		13b. TIME COVERED FROM TO	14. DATE OF REPORT (Year, Month, Day) 15 April 1989	15. PAGE COUNT 23
16. SUPPLEMENTARY NOTATION				
17. COSATI CODES			18. SUBJECT TERMS (Continue on reverse if necessary and identify by block number)	
FIELD	GROUP	SUB-GROUP	Electron Impact Ionization, Time-of-Flight, Mass Spectrometer, Spectrometer, Molecular Beams	
19. ABSTRACT (Continue on reverse if necessary and identify by block number)				
<p>A method is described for performing electron impact ionization time-of-flight mass spectrometry in a molecular beam apparatus. The method is a convenient way to optimize the performance of pulsed or continuous nozzle sources and can be used in conjunction with laser excitation. Mass spectra are produced either as analog waveforms or in a high repetition rate ion counting mode. The device can also be operated as a fast ionization gauge for time-resolved detection of pulsed beams.</p>				
20. DISTRIBUTION / AVAILABILITY OF ABSTRACT <input type="checkbox"/> UNCLASSIFIED/UNLIMITED <input checked="" type="checkbox"/> SAME AS RPT <input type="checkbox"/> DTIC USERS			21. ABSTRACT SECURITY CLASSIFICATION Unclassified	
22a. NAME OF RESPONSIBLE INDIVIDUAL			22b. TELEPHONE (Include Area Code)	22c. OFFICE SYMBOL

PREFACE

We acknowledge valuable discussions with G. S. Arnold, who is developing the miniature electron-impact ionization/time-of-flight mass spectrometer; and with J. A. Syage, who is developing the off-axis ionizer. We also thank R. L. Corbin for constructing the pulse decoupling transformer.



Accession For		
NTIS GRA&I	<input checked="checked" type="checkbox"/>	
DTIC TAB	<input type="checkbox"/>	
Unannounced	<input type="checkbox"/>	
Justification		
By		
Distribution/		
Availability Codes		
Avail and/or		
Dist		
A-1		

CONTENTS

PREFACE.....	1
I. INTRODUCTION.....	7
II. DESIGN.....	9
III. PERFORMANCE.....	17
APPENDIX.....	25
REFERENCES.....	27

FIGURES

1.	Schematic of the Molecular Beam Source and Ionization Region.....	10
2.	Ionizer Control Electronics.....	14
3.	Rendering of Scope Trace Exhibiting V_1 and GATE Pulses.....	15
4.	EI/TOFMS of a Pulsed Beam of 1% NH_3 in He.....	20
5.	EI/TOFMS of a Pulsed Beam of 5% HI in He.....	22

TABLE

1.	EI/TOFMS Parameters.....	11
----	--------------------------	----

1. INTRODUCTION

Time-of-flight mass spectrometry (TOFMS) is widely used in molecular beam research because it constitutes a nearly ideal detection system for experiments based on ionization by pulsed lasers.¹ Single-pass TOFMS is now a standard tool for spectroscopic studies of jet-cooled molecules and clusters,² and the addition of a reflecting field (in several different configurations) permits the investigation of a variety of ion fragmentation processes.^{3,4,5}

Electron-impact ionization (EI) is not often used in the present generation of molecular beam TOFMS experiments, despite the apparent value of EI as a universal beam diagnostic. With pulsed or with continuous nozzles, one typically needs a method for optimizing the beam intensity and the production (or suppression) of clusters. Laser ionization is at a disadvantage in this role precisely because of its selectivity. One does not always know in advance if there is an appropriate wavelength for resonant ionization, particularly in cases where the target molecule has all of its strong one-photon absorptions in the vacuum ultraviolet (VUV). Furthermore, laser ionization can be rather ill-suited for measuring a cluster size distribution if the cluster undergoes fast predissociation upon absorbing a single UV photon, as is apparently the case for nitric oxide.⁶ Because of ion fragmentation, EI cannot be regarded as a quantitative method for determining the size distribution of neutral clusters;⁷ however, it can provide a very useful lower bound on the degree of clustering in a given experiment.

In this report, we present a versatile and relatively simple method for implementing EI/TOFMS in a molecular beam apparatus. A single ionizer design is used for both EI and laser ionization and even permits the systems to be run simultaneously. The EI/TOFMS can be operated in a high repetition rate (> 20 kHz) ion-counting regime or in a low repetition rate analog regime using a transient recorder.

The design uses a grounded flight tube, which simplifies the vacuum hardware and is compatible with most laser TOFMS setups. The grid pulsing for EI is achieved with two low power pulse generators; one turns off the ion

extraction field, and the other turns on the electron beam during the same interval. Ion extraction takes place when both pulsers return to the quiescent state. Another novel feature of the current design is the capability to act as a continuous-sampling fast ion gauge (no mass discrimination) with 15 μ s rise time. Other variants on the basic design are discussed.

II. DESIGN

The primary reference for all designers of TOFMS devices during the last 30 years is the article by Wiley and McLaren⁸ that describes the use of a two-stage ion extraction system to achieve first-order space focusing. We adopt their concept as well as their notation throughout this work (see Appendix for definition of terms). Space focusing means that ions formed at the maximum distance from the detector ($2s_0 + d + D$) will acquire enough extra energy during the acceleration to just catch up with the ions formed at the minimum distance from the detector ($d + D$) by the time both ion groups reach the detector. Our design also benefits from the use of a collimated molecular beam to minimize the thermal spread in ion velocity in the direction parallel to the ion flight tube.¹

A schematic view of the EI/TOFMS is shown in Fig. 1. Typical operating parameters are listed in Table 1. The ionizer is operated in a Viton-sealed stainless steel vacuum chamber pumped by a liquid nitrogen- (LN-) trapped 10 in. diffusion pump (DP), or more recently by an 8 in. closed-cycle refrigerated cryopump. The base pressure is less than 4×10^{-8} Torr. The molecular beam is generated from pulsed or continuous nozzles in a separate chamber exhausted by an untrapped 20 in. DP. After the beam is skimmed, it enters a buffer chamber pumped by an untrapped 6 in. DP and passes through a final collimator into the ionizer chamber. After traveling through the ionizer, most of the beam is pumped away by a gas-catch arrangement using an LN-trapped 6 in. DP. For typical 10 Hz pulsed beam experiments, the pressure rise in the ionizer chamber as a result of the beam is less than 3×10^{-9} Torr. However, the pulsed beam number density at the ionizer can be in the 10^{13} cm^{-3} range for hydrogen or helium. The molecular beam diameter at the ionizer is about 3 mm.

The ionization region is between grids V_0 and V_1 for both laser ionization and EI. In the case of laser ionization, the photon beam enters from the direction orthogonal to both the molecular beam and the ion flight tube. The electron beam originates below the ionization region at a tungsten

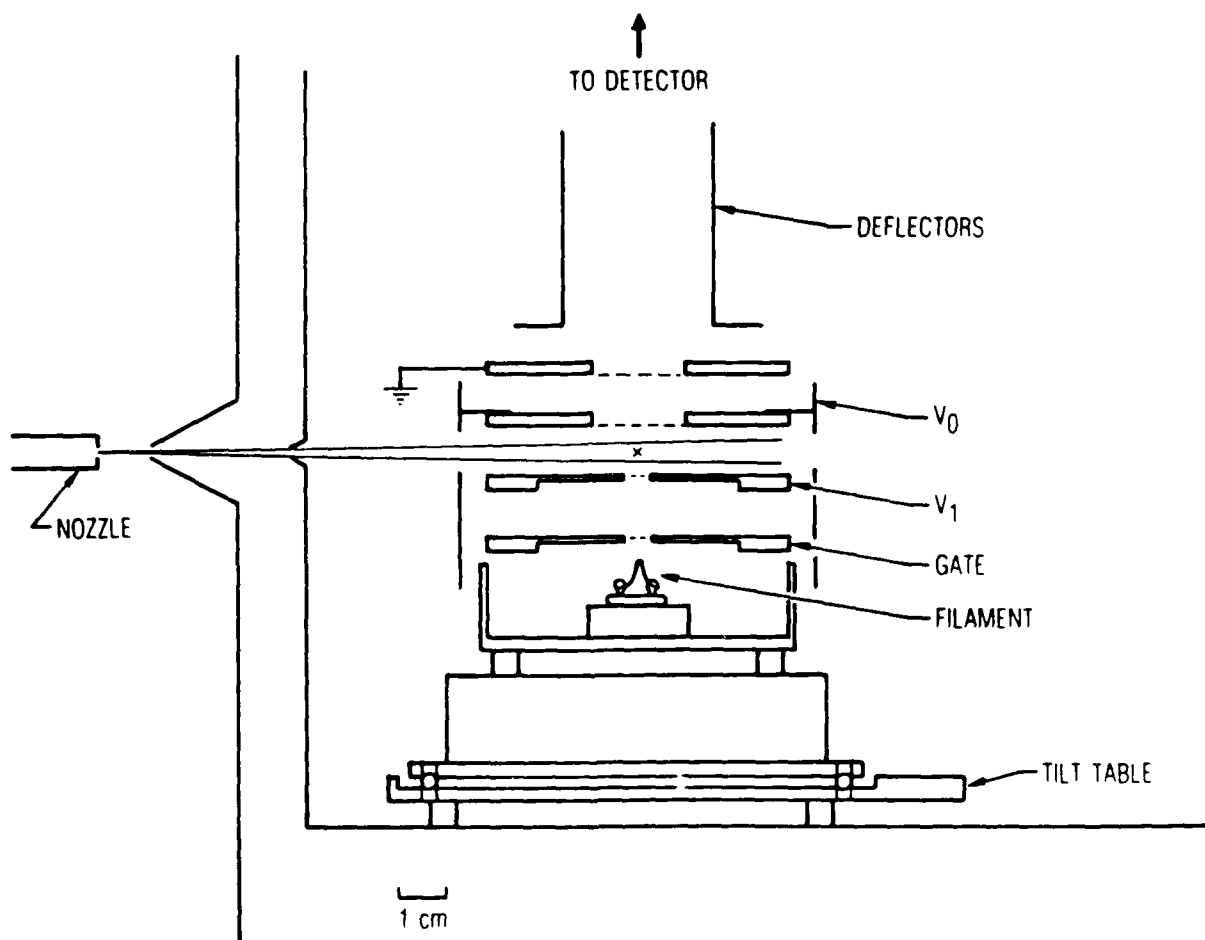


Fig. 1. Schematic of the Molecular Beam Source and Ionization Region

Table 1. EI/TOFMS Parameters (Notation from Ref. 8)

Geometry	Electric Field (V/cm)	Energy (eV)
D = 98.5 cm		$U_t = 1122$
d = 1.00 cm	$E_d = 1072$	$qdE_d = 1072$
$s_o = 0.50$ cm	$E_s = 100$	$qs_oE_s = 50$
$k_o = 22.443$	$T = 2.26 (M)^{1/2} \mu s$	
Voltages at 70 eV Impact Energy		
V_0	$= 1072$	
V_1	$= 1172 + 1072$ (pulse on)	
GATE	$= 972 + 1032$ (pulse on)	
FILAMENT	$= 1002$	

electron microscope filament and is collimated to a diameter of about 6 mm at the point where it intersects the molecular beam. A potential problem with this geometry is that the detector faces directly toward the filament and could be susceptible to spurious photon signals produced by the filament. This problem has never been observed in our setup, although it might occur if the flight tube were made very short.

The various grids are made from 70 line/in. electroformed copper mesh (with an optical transmission of 90%) that is stretched taut between stainless steel clamping rings. The grids are aligned and held parallel to one another by precision ceramic rods and spacers. A cylindrical shield made from a tantalum sheet is tied to V_0 and surrounds the ionizer in order to prevent the electron beam from being disturbed by stray electric fields. Holes in the shield permit passage of the laser and molecular beams. The entire ionizer is mounted on a simple tilt table so that the grids can be brought perpendicular to the flight tube axis. A kinematic mount using three sapphire spheres permits the ionizer to be removed for maintenance and to be repositioned precisely.

The current design assumes a grounded flight tube, which is the standard configuration for most laser ionization TOFMS. This design creates some complications for EI because of the need to apply time-varying fields to grids that are biased at high voltage. The pulse sequence that is required for the current EI configuration is described subsequently.

Ionization should take place in a field-free region to provide a well-defined impact energy and to permit proper space focusing. The ion extraction field then must be kept turned on long enough to sweep out all ions up to the maximum mass. To minimize the associated duty factor requirement, we adopt a scheme in which a pulse is applied to grid V_1 to turn off the extraction field. When this pulse relaxes, the field turns back on, and the ions begin their flight to the detector. Thus, there is no upper limit to the mass scale, because the extraction field stays on indefinitely after the ions are formed. During the time that the pulse to grid V_1 has turned off the extraction field (typically 1000 ns), a second pulse of around 600 ns duration

is applied to the GATE grid to admit the electrons into the ionization region. The electron beam needs to be turned off at other times to prevent ionization and extraction from taking place continuously. (In Section III, we discuss how this effect can be exploited to turn the TOFMS into a fast ion gauge.)

The use of a grounded flight tube, while facilitating the construction of the drift region and detector, requires that pulses be applied to the V_1 and GATE grids when they are at high voltage, as specified in Table 1. This can be accomplished either by floating a pulse generator or by decoupling it from high voltage using a transformer or capacitor. The former approach permits good pulse fidelity at the cost of some extra construction, whereas the latter approach is easy to implement but degrades the pulse shape. We decided to float the V_1 pulse generator in a plexiglass isolation box along with the filament power supply. Because the shape of the pulse used to turn the electron beam on and off is not critical, the GATE pulse generator is decoupled from high voltage using a small ferrite core transformer. The transformer is wound with a turn ratio of PRI:SEC = 8:36 and provides at least 1000 V of isolation between primary and secondary.

A schematic of the ionizer control circuit is shown in Fig. 2, and the resultant waveforms are shown in Fig. 3. To minimize reflections, the V_1 pulse passes into the chamber via a constant-impedance floating BNC feedthrough, and the coaxial cable is terminated by connection to a 50 Ω resistor directly at the V_1 grid. This cable must be carefully insulated because the shield (as well as the inner conductor) is floated at high voltage. The GATE pulse is terminated outside the vacuum with a 5 k Ω potentiometer that is adjusted to optimize the pulse shape. Typically the ferrite core steps up the amplitude of the 25 V drive pulse by a factor of 2 to 3. The GATE pulse is delivered from the terminator to the grid via a single unshielded lead wire, which seems to minimize reactance and improve the pulse shape. For both the V_1 and GATE pulses, the cables should be as short as possible (certainly less than 2 m) to reduce reflections.

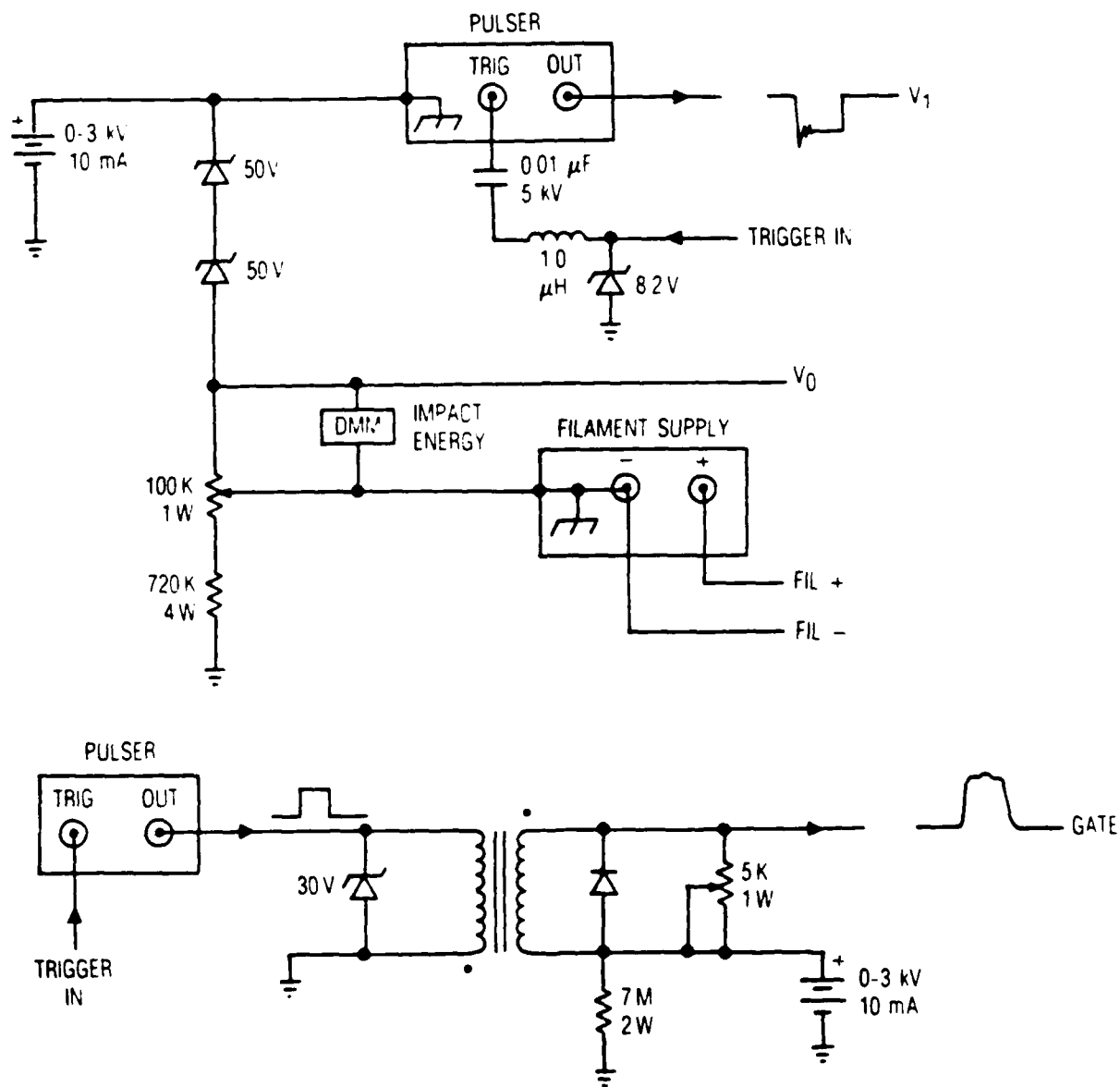


Fig. 2. Ionizer Control Electronics

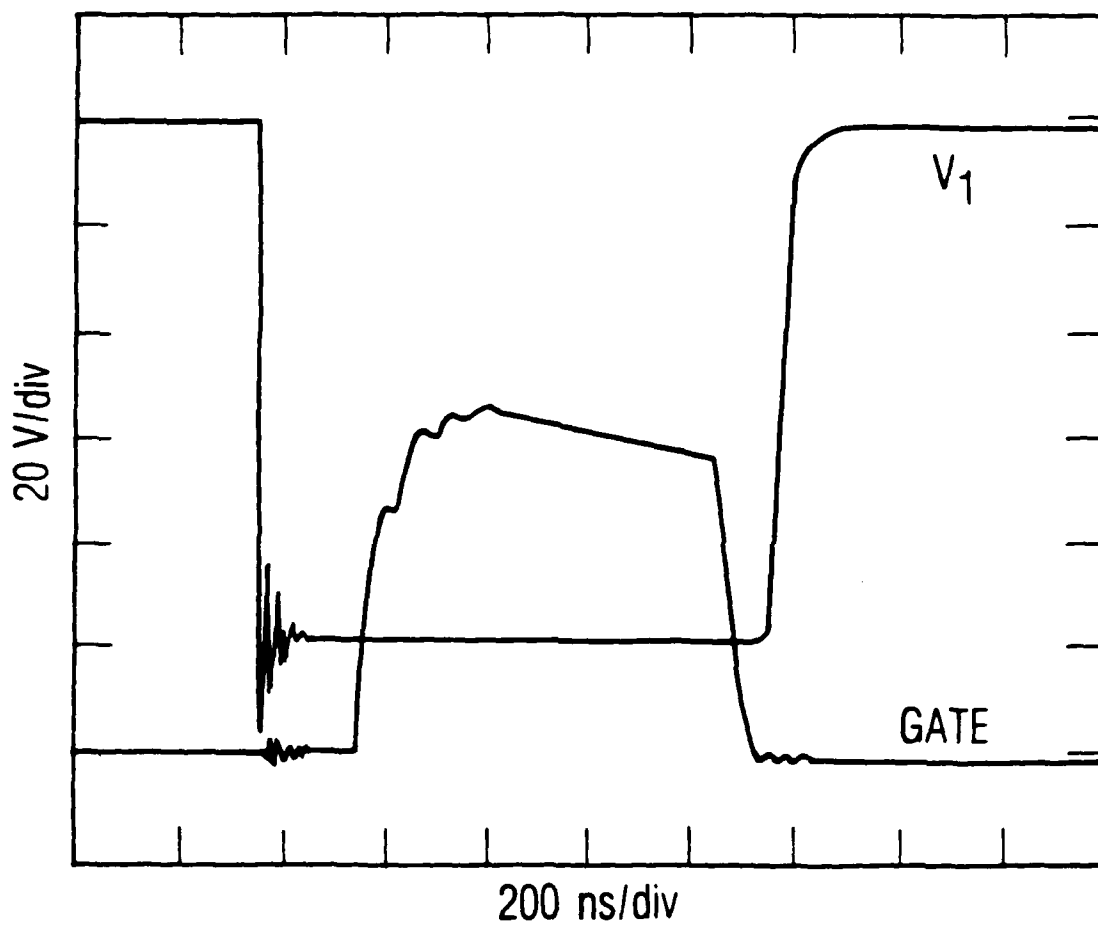


Fig. 3. Rendering of Scope Trace Exhibiting V_1 and GATE Pulses

The detector is a 40 mm diameter dual microchannel plate with a plain metal anode (nominally at ground) as the collector. The large active area of this detector helps to maximize the collection efficiency over the full range of masses. A standard problem for molecular beam TOFMS is that a portion of the mass range fails to hit the detector because of the perpendicular drift velocity imparted by the molecular beam. Several schemes have been proposed to correct this difficulty, including a time-varying deflecting field¹ and an electrostatic lens² to refocus the ions. We have made a few attempts to refocus the ions using an electrostatic lens, but we generally find that a small DC deflecting field is the best solution for our configuration. It has been suggested that nearly perfect collection efficiency independent of mass could be achieved by immersing the ion flight tube and ionizer in a solenoidal magnetic field.* However, we are unaware of any attempts to implement this approach. The disadvantage of our large-area detector in its present form is that the impedance mismatch inherent in the plain metal anode results in ringing in the output pulse. A coaxial-cone anode having 50 Ω impedance⁹ can eliminate the ringing, although it usually entails a reduction in the collection area of the detector. A possible exception to this reduction is provided by the variable-impedance coaxial-cone anode.¹⁰

* J. A. Syage and R. Rianda, personal communication.

III. PERFORMANCE

The EI/TOFMS can be cycled at rates from a single shot to 5 kHz using the pulse waveforms shown in Fig. 3. Higher rates are achievable (> 20 kHz) if the V_1 and GATE pulses are narrowed to avoid exceeding the maximum duty factor (0.5%) of the existing V_1 pulse generator. This means that fewer ions are produced on each shot, because the electron beam is turned on for a shorter period of time. At a low repetition rate, the electron beam, in principle, could be turned on for as long as 2 μ s to improve ionization efficiency; beyond ~ 2 μ s, the first ions to be formed will be carried out of the extraction volume by the molecular beam velocity.

Two modes of signal recovery are possible: the analog mode and the ion counting mode. The analog mode applies when the ionizer is running at high emission current and many ions (10^1 - 10^4 per mass) are produced on each shot. A well-developed analog TOFMS waveform is then available on each shot for processing by a transient recorder or boxcar averager. The analog mode is used for all pulsed beam experiments because of the intrinsically low (< 100 Hz) repetition rate. In the analog mode, the dynamic range, defined as the ratio of the largest to the smallest mass peak detected on a single shot, is limited either by the signal-to-noise ratio (500:1 is typical) or by the number of bits in the transient recorder (usually 255:1).

For continuous nozzle beams, an alternative ion counting mode can be used to extend the dynamic range. The TOFMS is cycled at 20 kHz or more, and the filament current is reduced so that less than one ion per shot is detected at any particular mass. Thus gated counting techniques can be used to achieve a dynamic range of greater than 2000:1 in only a few seconds of counting. If the probability of detecting a given ion mass is 0.1 per shot, then the probability of detecting two ions at that mass is 0.01 per shot, which amounts to a 10% error in the observed count rate because of double ion events being registered as single counts. We generally find 10% to be an acceptable error level; therefore, we try to keep the maximum count rate for a given mass to around 2000 Hz. The most effective method for recovering the data in the ion

counting mode seems to be via a high resolution multihit, time-to-digital converter.¹¹ We have not implemented this method.

The sensitivity of the current ionizer can be gauged using a number of methods that are employed for determining the absolute number density (at the ionizer) of pulsed or continuous beams. The most straightforward method is to calibrate the ionizer by increasing the main chamber background pressure with a known amount of bleed gas and correcting the observed signals for the assumed ionization volume difference between molecular beam and bleed. The evidence suggests that at high filament current (2.65 A) and 70 eV impact energy, we are able to ionize approximately 1 out of 10^7 molecules in the volume defined by the intersection of the molecular beam (~ 3 mm diameter) and the electron beam (~ 6 mm diameter). This means that the minimum detectable number density in this volume is around 10^8 cm^{-3} .

The degree of sensitivity is quite adequate for current use but could be improved by several routes. The filament could be placed closer to the ionization volume and could be gated on for the full 2 μs , as previously described. It might be more effective to replace the pointlike hairpin filament source with a tungsten dispenser-cathode impregnated with barium oxide. This modification would be expected to increase the electron beam current from its present 10^{-4} A range to the 10^{-2} A range, if the ionizer voltage divider shown in Fig. 2 is also beefed up to permit higher emission current. A possible drawback is that as the barium slowly evaporates from the cathode, some of it could be deposited on the microchannel plate detector. The use of a solenoidal magnetic field was mentioned previously as a possible means for overcoming the perpendicular drift velocity of the ions. The magnetic field might also help to collimate the electron beam and thereby improve the ionization efficiency.

The practical mass resolution in this EI/TOFMS is governed by several factors. The use of first-order space focusing and a collimated molecular beam eliminates two of the largest potential sources of mass peak linewidth.⁸ Tuning up for optimal resolution is a simple procedure. The DC voltages on V_0 , V_1 , GATE, and FILAMENT are set to their respective calculated

values, as shown in Table 1, and are checked using a high voltage probe and digital multimeter. Then, while the mass spectrum of a molecular beam is observed, the amplitude of the V_1 pulse is carefully tweaked in order to narrow the mass peak as much as possible. Without this final adjustment, one cannot be sure that the V_1 pulse exactly cancels out the ion extraction field during the time that the electron beam is turned on. Any residual field tends to give a head start to some ions and to broaden the mass peaks.

When helium beams are run, the intrinsic width of the unsmoothed anode pulses for mass 4 (in analog mode) is 7 ns full-width, half maximum (FWHM) with ringing that extends to approximately 40 ns beyond the peak. The ringing is a result of the unmatched anode, as just described. Because the microchannel plate is expected to have a subnanosecond rise time,⁹ we attribute the observed 7 ns width to the finite switch-on time of the ion extraction field (40 ns, 10-90%) or to less than perfect space focusing. If the mass resolution were limited only by this 7 ns width, we could expect to achieve an $M/\Delta M$ well above 2000. However, in practice, some other factors come into play. The anode pulses for energetic fragment ions can be much wider than 7 ns because of the relatively modest extraction field, $E_s = 100$ V/cm. Furthermore, we generally find it advisable to use a smoothing amplifier that broadens all the mass peaks to approximately 20 to 30 ns FWHM and quenches the anode ringing fairly effectively. Besides permitting easier viewing on a scope, smoothing is mandatory if the waveform is to be processed by a transient recorder, because these devices usually do not sample faster than 5 ns per point. If we assume that adjacent mass peaks are just resolvable when the FWHM equals the spacing between peaks, a pulse width of 20 to 30 ns corresponds to a maximum resolvable mass of 1400 to 3200 amu for parent ions. This resolution criterion is strictly applicable only when the two adjacent mass peaks are of equal intensity, a situation that rarely occurs.

As a demonstration of the realistically achievable capabilities of this EI/TOFMS, Fig. 4 exhibits the mass spectrum that results when 1% NH_3 in He at 60 psig is expanded through a 0.5 mm diameter pulsed nozzle at room temperature. The electron impact energy is 70 eV; a 20 V/cm deflecting field

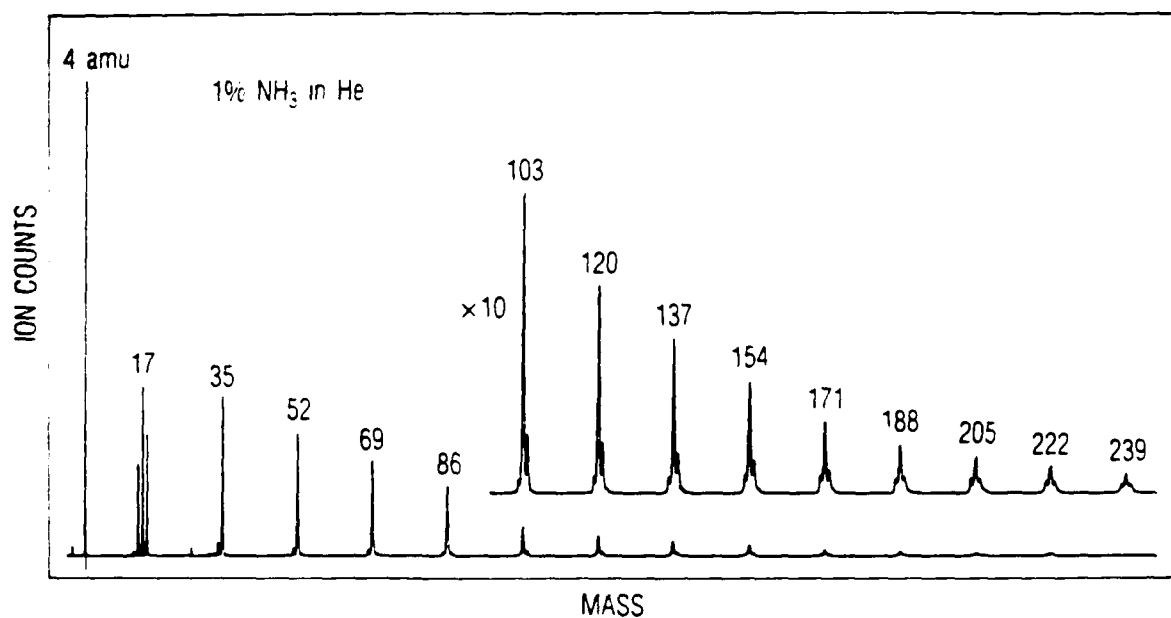


Fig. 4. EI/TOFMS of a Pulsed Beam of 1% NH₃ in He. The beam is expanded from 60 psig through a 0.5 mm diameter nozzle at 305 K. The mass of the main peak in each group is given in atomic mass units.

is applied to bring out the higher masses. The spectrum consists of a 1000 shot average accumulated in 100 s with a 10,000 point record length at 5 ns per point. The results are similar to those reported recently by Shinohara, Nishi, and Washida,¹² who used a continuous nozzle beam and a quadrupole mass spectrometer. The major cluster ion mass peaks (35,52,69,... amu) are assigned to the $(\text{NH}_3)_{n-1}\text{NH}_4^+$ fragment, where n equals 2 to 14 in the portion of the spectrum plotted in Fig. 4. On either side of the main mass are smaller peaks that are assigned to $(\text{NH}_3)_n^+$ and to $(\text{NH}_3)_{n-2}\text{OH}_2\text{NH}_4^+$. The latter fragment is evidently the result of a water impurity in the sample. Note that adjacent masses are separable out to at least 230 amu, which gives a good idea of the resolution under realistic conditions.

Figure 5 is the mass spectrum of a beam containing 5% HI in He expanded from 10 psig through a 0.5 mm diameter pulsed nozzle. The impact energy is 70 eV, the deflecting field is 10 V/cm, and the spectrum is averaged for 500 shots at 5 ns per point. The digitized peak widths are 30 ns FWHM for the HI^+ parent ion and 42 ns FWHM for the I^+ fragment, whereas the corresponding widths of the unsmoothed anode pulses are 15 ns for HI^+ and 40 ns for I^+ .

Several variants on the basic operating procedure are possible. Laser excitation or ionization may be used simultaneously with the EI/TOFMS. If the laser pulse arrives within the duration of the V_1 pulse, then the laser and EI mass spectra will be referenced to the same time zero. If the laser is fired before or after the V_1 pulse, then the two mass spectra will be out of phase. Experiments in which EI is used to probe the products of a laser-induced process are possible, if the laser is capable of exciting a significant fraction of the molecules in the volume sampled by the electron beam. In cases where only laser ionization is desired, we typically use a different grid biasing arrangement from that given in Table 1: the ion energy and extraction field are increased to 2244 eV and 200 V/cm to improve collection efficiency.

Another variant is the fast ion gauge mode, in which the electron beam and ion extraction field are held on continuously, and ions are detected without mass discrimination. The required positive voltages relative to

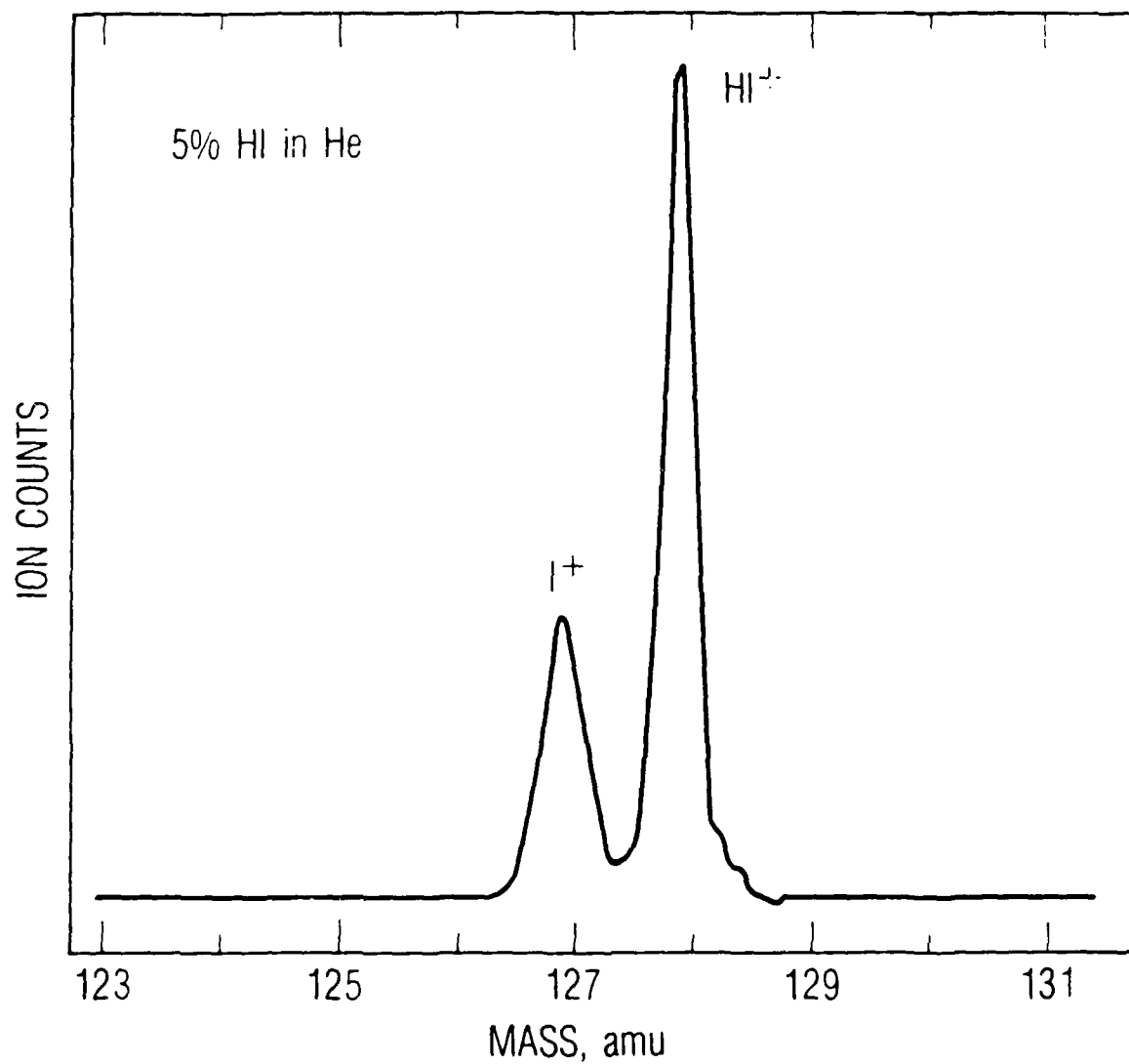


Fig. 5. EI/TOFMS of a Pulsed Beam of 5% HI in He. The beam is expanded from 10 psig through a 0.5 mm diameter nozzle at 305 K.

ground are $V_0 = 800$ V, $V_1 = \text{GATE} = 900$ V, and $\text{FILAMENT} = 780$ V. The detector is operated at rather low gain ($< 10^5$) to prevent the anode current from exceeding 10% of the 15 μA strip current. The anode is connected to a 10^6 V/A current amplifier with 15 μs rise time, and the output is available for scope viewing. The fast ion gauge mode is very useful for optimizing the pulsed valve behavior and for setting the delay between the triggering of the valve and the laser or EI firing.

Two extensions of the basic EI/TOFMS design are presently under development. The first extension is a miniature version with a nongrounded drift tube that simplifies the grid pulsing considerably. This device is intended to be a compact, low-cost alternative to a quadrupole mass filter for detecting high molecular weight (500 amu) hydrocarbons at moderate mass resolution. The second extension is an off-axis ionizer that is intended to detect high velocity photofragments as they emerge from the molecular beam. Neutral fragments will pass through a grid into a high current electron beam, and from there, will be swept to the detector when the extraction field turns on.

APPENDIX

A summary of the notation used by Wiley and McLaren⁸ is provided in this Appendix. Ionization and the first stage of acceleration take place between two grids (labeled V_0 and V_1) that are separated by a distance $2s_0$; the position s_0 is halfway between the grids. The second stage of acceleration takes place over a distance d between grid V_1 and a grid at the drift tube potential. Distance D is the spacing between this latter grid and the detector. The total ion flight distance is $s + d + D$, where $0 \leq s \leq 2s_0$. The electric fields in the two acceleration regions are E_s and E_d . For an ion at s_0 that is initially at rest, the kinetic energy in the drift tube is

$$U_t = q s_0 E_s + q d E_d = k_0 q s_0 E_s$$

where

$$k_0 = (s_0 E_s + d E_d) / s_0 E_s$$

and the total flight time is

$$T(\mu s) = 0.7199 \sqrt{\frac{M \text{ (amu)}}{U_t \text{ (eV)}}} (2s_0 \sqrt{k_0} + \frac{2 d \sqrt{k_0}}{1 + \sqrt{k_0}} + D)$$

where s_0 , d , and D are in centimeters. The first-order space focusing condition is obtained by setting $dT/ds = 0$, resulting in the following:

$$D = 2s_0 k_0^{3/2} \left[1 - \left(\frac{1}{k_0 + \sqrt{k_0}} \right) \frac{d}{s_0} \right]$$

Our approach is to select the three distance parameters and to solve this expression numerically for k_0 , thus determining the required voltages.

REFERENCES

1. D. M. Lubman and R. M. Jordan, Rev. Sci. Instrum. 56, 373 (1985); also, J. D. Pinkston, M. Rabb, J. T. Watson, and J. Allison, Rev. Sci. Instrum. 57, 583 (1986).
2. E. Carrasquillo, T. S. Zwier, and D. H. Levy, J. Chem. Phys. 83, 4990 (1985).
3. M. A. Johnson, M. L. Alexander, and W. C. Lineberger, Chem. Phys. Lett. 112, 285 (1985).
4. O. Echt, P. D. Dao, S. Morgan, and A. W. Castleman, Jr., J. Chem. Phys. 82, 4076 (1985).
5. H. Kuhlewind, H. J. Neusser, and E. W. Schlag, J. Chem. Phys. 82, 5452 (1985).
6. K. Sato, Y. Achiba, and K. Kimura, Chem. Phys. Lett. 126, 306 (1985).
7. U. Buck and H. Meyer, J. Chem. Phys. 84, 4854 (1986).
8. W. C. Wiley and I. H. McLaren, Rev. Sci. Instrum. 26, 1150 (1955).
9. J. L. Wiza, Nucl. Instrum. Meth. 162, 587 (1979).
10. M. G. White, R. A. Rosenberg, G. Gabor, E. D. Poliakoff, G. Thornton, S. H. Southworth, and D. A. Shirley, Rev. Sci. Instrum. 50, 1268 (1979).
11. D. Ren, T. T. Tsong, and S. B. McLane, Rev. Sci. Instrum. 57, 2543 (1986).
12. H. Shinohara, N. Nishi, and N. Washida, J. Chem. Phys. 83, 1939 (1985).

LABORATORY OPERATIONS

The Aerospace Corporation functions as an "architect-engineer" for national security projects, specializing in advanced military space systems. Providing research support, the corporation's Laboratory Operations conducts experimental and theoretical investigations that focus on the application of scientific and technical advances to such systems. Vital to the success of these investigations is the technical staff's wide-ranging expertise and its ability to stay current with new developments. This expertise is enhanced by a research program aimed at dealing with the many problems associated with rapidly evolving space systems. Contributing their capabilities to the research effort are these individual laboratories:

Aerophysics Laboratory: Launch vehicle and reentry fluid mechanics, heat transfer and flight dynamics; chemical and electric propulsion, propellant chemistry, chemical dynamics, environmental chemistry, trace detection; spacecraft structural mechanics, contamination, thermal and structural control; high temperature thermomechanics, gas kinetics and radiation; cw and pulsed chemical and excimer laser development including chemical kinetics, spectroscopy, optical resonators, beam control, atmospheric propagation, laser effects and countermeasures.

Chemistry and Physics Laboratory: Atmospheric chemical reactions, atmospheric optics, light scattering, state-specific chemical reactions and radiative signatures of missile plumes, sensor out-of-field-of-view rejection, applied laser spectroscopy, laser chemistry, laser optoelectronics, solar cell physics, battery electrochemistry, space vacuum and radiation effects on materials, lubrication and surface phenomena, thermionic emission, photo-sensitive materials and detectors, atomic frequency standards, and environmental chemistry.

Computer Science Laboratory: Program verification, program translation, performance-sensitive system design, distributed architectures for spaceborne computers, fault-tolerant computer systems, artificial intelligence, micro-electronics applications, communication protocols, and computer security.

Electronics Research Laboratory: Microelectronics, solid-state device physics, compound semiconductors, radiation hardening; electro-optics, quantum electronics, solid-state lasers, optical propagation and communications; microwave semiconductor devices, microwave/millimeter wave measurements, diagnostics and radiometry, microwave/millimeter wave thermionic devices; atomic time and frequency standards; antennas, rf systems, electromagnetic propagation phenomena, space communication systems.

Materials Sciences Laboratory: Development of new materials: metals, alloys, ceramics, polymers and their composites, and new forms of carbon; non-destructive evaluation, component failure analysis and reliability; fracture mechanics and stress corrosion; analysis and evaluation of materials at cryogenic and elevated temperatures as well as in space and enemy-induced environments.

Space Sciences Laboratory: Magnetospheric, auroral and cosmic ray physics, wave-particle interactions, magnetospheric plasma waves; atmospheric and ionospheric physics, density and composition of the upper atmosphere, remote sensing using atmospheric radiation; solar physics, infrared astronomy, infrared signature analysis; effects of solar activity, magnetic storms and nuclear explosions on the earth's atmosphere, ionosphere and magnetosphere; effects of electromagnetic and particulate radiations on space systems; space instrumentation.

END

FILMED

6-89

DTIC